Small-angle attraction in the tilt illusion

Ayşe Akgöz
McGill Vision Research, Department of Ophthalmology, Montréal General Hospital, Cedar Ave. Rm. L11.512, Montréal, Québec, H3G 1A4, Canada

Elena Gheorghiu
University of Stirling, Department of Psychology, Stirling, FK9 4LA, Scotland, United Kingdom, Canada

Frederick A. A. Kingdom
McGill Vision Research, Department of Ophthalmology, Montréal General Hospital, Cedar Ave. Rm. L11.512, Montréal, Québec, H3G 1A4, Canada

The tilt illusion (TI) describes the phenomenon in which a surround inducer grating of a particular orientation influences the perceived orientation of a central test grating. Typically, inducer-test orientation differences of 5 to 40 degrees cause the test orientation to appear shifted away from the inducer orientation (i.e. repulsion). For orientation differences of 60 to 90 degrees, the inducer typically causes the test grating orientation to appear shifted toward the inducer orientation, termed here "large-angle" attraction. Both repulsion and large-angle attraction effects have been observed in contrast-modulated as well as luminance-modulated grating patterns. Here, we show that a secondary, "small-angle" 0 to 10 degrees attraction effect is observed in contrast-modulated and orientation-modulated gratings, as well as in luminance-modulated gratings that are relatively low in spatial frequency, low in contrast, or contain added texture. The observed small-angle attraction, which can exceed in magnitude that of the repulsion and large-angle attraction effects, is dependent on the spatial phase relationship between the inducer and test, being maximal when in-phase. Both small-angle attraction and repulsion effects are reduced when a gap is introduced between the test and inducer. Our findings suggest that small-angle attraction in the TI is a result of assimilation of the inducer pattern into the receptive fields of neurons sensitive to the test.

Introduction

The tilt illusion, or TI, first reported by Gibson (1937), is the phenomenon in which the perceived orientation of a central test line or grating is altered by the presence of a surround or inducing line/grating with a different orientation (see review by Clifford, 2014). Examples of the TI are shown in Figure 1 for various types of grating pattern. The figure includes not only luminance-defined (LM) or "first-order" gratings but two types of texture-defined, or "second-order" gratings (Graham, 2011): contrast-modulated (CM), for which the TI has been previously demonstrated (Badcock & Hutchison, 1998; Smith, Clifford, & Wenderoth, 2001), and orientation-modulated (OM), for which, to our knowledge, it has not. In the classical version of the TI with LM stimuli, an obliquely tilted inducer grating causes the perceived orientation of a vertical test grating to be slightly tilted away from that of the inducer. This "repulsive" interaction occurs maximally for inducer-test orientation differences of around 15 to 20 degrees. Inducer grating orientation differences of 70 degrees or more typically cause the test grating to appear tilted toward the inducer orientation, with the maximum effect observed between 75 and 80 degrees (Over, Broerse, & Crassini, 1972; Wenderoth & Johnstone, 1987; Clifford, 2014) and termed the "indirect" effect. Here, we use the term "large-angle attraction" for the indirect effect to distinguish it from a secondary, small-angle attraction effect that is the subject of the present study.

The classical explanation of the repulsive effect in the TI is lateral inhibition between orientation selective neurons (Wallace, 1969; Blakemore, Carpenter, & Georgeson, 1970; Georgeson, 1973; Tolhurst & Thompson, 1975; Ringach, 1998; Clifford, 2014; Clifford, Wenderoth & Spehar, 2000). For the large-angle attractive effect, disinhibition, or "inhibition of the inhibition" (Clifford, 2014) and orientation constancy (Wenderoth & Johnstone, 1987; Wenderoth & Johnstone, 1988) have been suggested as possible explanations, to which we shall return.

In this communication, we systematically explore the TI at small angles, specifically in the region 0

Citation: Akgöz, A., Gheorghiu, E., & Kingdom, F. A. A. (2022). Small-angle attraction in the tilt illusion. *Journal of Vision*, *22*(8):16, 1–12, https://doi.org/10.1167/jov.22.8.16.

https://doi.org/10.1167/jov.22.8.16 Received January 28, 2022; published July 28, 2022 ISSN 1534-7362

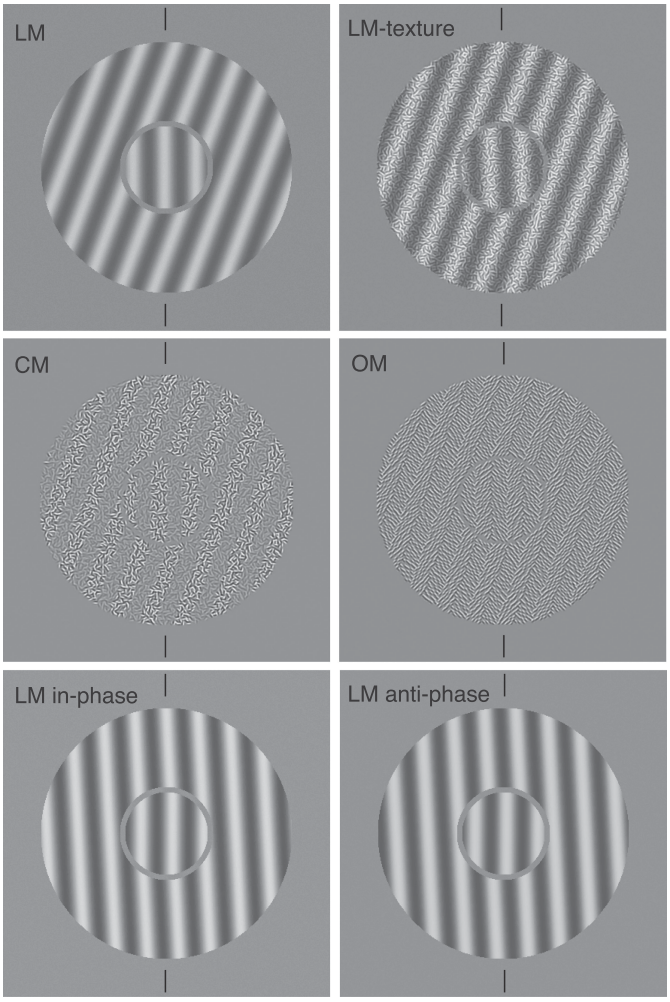

Figure 1. Tilt illusion in luminance modulated (LM), luminance modulated with uniform texture (LM-texture), contrast modulated (CM) and orientation-modulated (OM) gratings. In the top and middle panels, the bars in the central test area are physically vertical (0 degrees), but for most observers appear tilted slightly counterclockwise due to the +20 degree surround, when compared to the vertical reference lines above and below. The bottom panel shows the in-phase and anti-phase conditions for a vertical test with a –3 degree surround.

to 10 degrees, to determine if there is a secondary, small-angle attraction effect that is distinct from the large-angle attraction effect discussed above. Only a small number of studies have delved into the TI in the 0 to 10 degrees range and of those that have, only two to our knowledge have found at least some evidence for small-angle attraction, albeit only in very specific circumstances. Takeo, Watanabe, and Clifford (2020) found small-angle TI attraction in LM gratings with 10 degree inducers, but only at very short stimulus durations of 20 ms or less. Mareschal, Morgan, & Solomon (2010), using stimuli comprised of a central Gabor test surrounded by four Gabor flankers found small-angle attraction for 5 to 10 degree flanker-test differences, but only at an eccentricity of 10 degrees.

Some non-TI studies lend support to the possibility of small-angle attraction in the TI. Using orientationally narrowband noise patterns, Blake, Holopigian, and Jauch (1985) measured the perceived orientation of a test noise pattern in the context of a superimposed mask noise pattern. They found that at large mask-test angles (>10 degrees) the test orientation appeared rotated away from the mask orientation, in keeping with the repulsion effect in the TI. However, when mask-test angles were <10 degrees the test orientation appeared rotated toward the mask orientation, showing attraction. Given that overlay masking is likely underpinned by similar mechanisms to those mediating the TI, we might expect an attraction effect in the TI for small inducer-test angles. Further support for the possibility of small-angle attraction in the TI comes from a study by Motoyoshi and Kingdom (2003), in which subjects discriminated noise patterns with an even distribution of orientation energy from ones with orientation energy that was sinusoidally modulated across orientation (i.e. rather than across space or time). They found that sensitivity was bandpass with respect to orientation frequency and modeled their results with an orientation-based filter that involved facilitatory (i.e. attractive) interactions between similar orientations, and inhibitory (i.e. repulsive) interactions between dissimilar orientations.

Besides the fact that few studies have studied in any detail the TI at small angles, one reason why attraction in this region might have proved elusive is that the spatial-phase relationship between the inducer and test has not been an independent variable. If small-angle attraction were to be dependent on colinear interactions between the inducer and test it might be expected to be dependent on their spatial-phase relationship. Moreover, most TI studies have limited themselves to LM stimuli, whereas it is possible that small-angle attraction is primarily a feature of second-order stimuli.

To this end, we have measured the TI at small angles using modulations in which the spatial phases of the inducer and test have either been in-phase or anti-phase, using both first-order LM and second-order CM and OM stimuli.

Methods

Observers

The three authors acted as observers in all experiments. An undergraduate volunteer took part in experiment 5. All subjects were emmetropic or wore corrective lenses. All experiments were conducted in

accordance with the Declaration of Helsinki (2008, version 6) and the Research Institute of the McGill University Health Centre (RI-MUHC) Ethics Board. Observer initials on graphs have been anonymized in accordance with requirements of the (RI-MUHC) Ethics Board.

Stimuli – generation and display

Stimuli were generated by a VISAGE graphics card (Cambridge Research Systems, Riverside, Kent, UK) driven by a Dell Precision PC and displayed on a Sony Trinitron F500 flatscreen monitor running at 120 Hz frame rate and with spatial resolution of 640 × 480 pixels. The mean luminance of the monitor was 40 cd/m^2. Viewing distance was 100 cm. Psychophysics software was written in C and C++ and contained embedded VISAGE routines.

Example stimuli are shown in Figure 1. Each stimulus is composed of a central test region of 4 degrees in diameter and a surround annulus 12 degrees in diameter, separated by a gap of 0.25 degrees. Modulation frequencies of four, eight, and 16 cycles per image (cpi) were used, corresponding to, respectively, 0.33, 0.66, and 1.32 cycles per degree (cpd). The absolute spatial phases of the stimuli were randomized on each trial, but the spatial-phase relationship between the inducer and test was set either to "in-phase" or "anti-phase" (see Figure 1 bottom panel). These two spatial-phase relationships, each of which was defined in relation to the randomized absolute phases of the inducer and test, must be understood in context. When the inducer and test are both vertical, the in-phase condition results in colinear alignment of bars of the same polarity, whereas the anti-phase condition results in colinear alignment of bars of opposite polarity. However, as the orientation difference between the inducer and test increases the bars in both phase conditions become increasingly misaligned because of the constraints imposed by the geometry of the stimulus and the fact that the spatial frequencies of the inducer and test modulations are always equal. To preserve colinear alignment across all inducer-test orientation differences would have necessitated setting the inducers and tests to spatial frequencies that differed increasingly with inducer orientation, thereby compromising the constraint of equal inducer-test spatial frequencies.

The LM stimulus, as with the LM component of the LM-texture stimulus (see Figure 1), was sinusoidally modulated with a contrast of 0.25 in the main experiment (experiment 1) but with a lower contrast in experiment 4, as detailed below. The CM and OM stimuli were square-wave modulated to maximize their modulation energy, but we chose not to use square-wave modulation for the LM stimuli to avoid aliasing at the edges.

The OM, CM, and LM-texture stimuli were composed of 3600 odd-symmetric Gabor micropatterns with a spatial frequency of 6.0 cpd, a bandwidth at half-height of 1.5 octaves, and an envelope diameter of 5 standard deviations (SDs). Gabors were randomly positioned with the constraint that adjacent Gabors were a minimum of 1.7 SDs apart. The orientations of the Gabors were selected from 1400 templates distributed evenly across the 360 deg range, giving an orientation precision of 0.25 degrees.

In the CM stimuli the orientations of the Gabors were random, and their contrasts square-wave modulated with an amplitude of 0.165 and a mean contrast of 0.33. In the OM stimuli, the Gabor contrasts were 0.33 and their orientations square-wave modulated with an amplitude of 45 degrees around a mean orientation of 90 degrees (horizontal).

In the LM-texture stimuli, the Gabor texture and LM components were displayed on separate pages of video memory. The Gabor contrasts on one page were sinusoidally modulated with an amplitude of 0.333 and a mean contrast of 0.666, resulting in a peak-to-trough contrast ratio of three. The LM stimulus on the other page had a modulation contrast of 0.5, resulting also in a peak-to-trough luminance ratio of three. The Gabor-contrast and LM components were combined in-phase in order to simulate shading of a spatially uniform contrast texture (Schofield, Heese, Roek, & Georgeson et al., 2006). The combination was achieved by page-alternating the two modulations at 120 Hz. This halved all contrasts reaching the eye and thus the LM-texture had an LM contrast of 0.25 and Gabor contrast of 0.333.

Procedure: Interleaved inducer orientations

We used a new method for measuring the TI: interleaving inducers with opposite signs of orientation during a session. The advantage of this method over previous single-inducer protocols is twofold. First, it reduces the likelihood of any bias for responding according to perceived inducer orientation: all observers reported that during each session they were largely unaware on each trial as to whether the inducer orientation was oriented clockwise or anticlockwise. Second, the method allows one to take into account any bias for responding clockwise more than anticlockwise or vice versa. By taking the difference between the estimated point-of-subjective-vertical (PSV), for the two opposite-sign inducer orientations (see below) this type of response bias is removed.

In all experiments, the observer was presented on each trial with a TI stimulus and tasked with

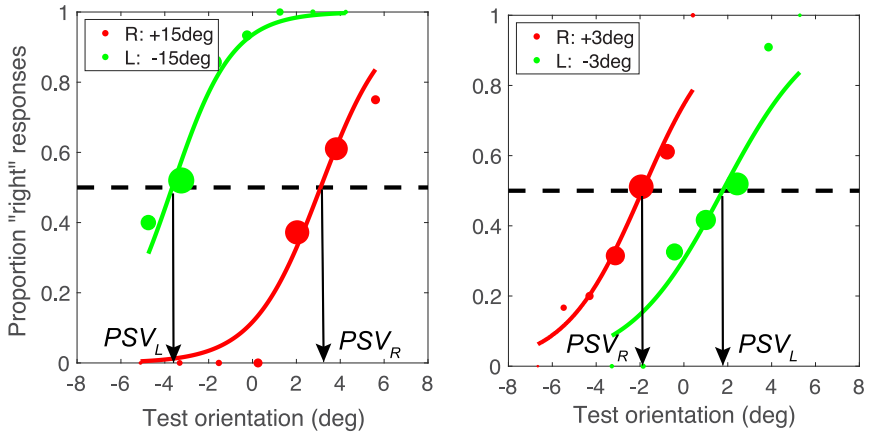

Figure 2. Example psychometric functions (PFs) and the method for estimating the point-of-subjective-vertical (*PSV*) from the interleaved ± inducer orientations. Each PF plots the proportion of right, or clockwise responses as a function of the orientation of the test pattern. The diameter of each data point is proportional to the number of trials in each "bin." Continuous curves are Logistic function fits. Red is for the clockwise inducer, and green for the anticlockwise inducer. The left graph gives the PFs for observer 2's LM ±15 degrees inducer condition; the right graph gives the PFs for observer 3's OM ±3 degrees inducer condition. Note the reversal in the order of the two PFs in the two graphs. The *PSV* is calculated as (PSV_R-PSV_L)/2. The resulting positive *PSV* in the left graph indicates repulsion while the negative *PSV* in the righthand graph indicates attraction.

indicating whether the test modulation appeared oriented clockwise or anticlockwise from vertical. Two black lines above and below the stimulus provided a reference to vertical (see Figure 1). During each session of 100 trials, two opposite-sign inducer orientations (e.g. +20 degrees and -20 degrees) were presented in random order (50 trials each), and the test orientations were determined by separate staircases for each inducer orientation. A "clockwise" response resulted in a shift in test orientation away from clockwise for the next trial, whereas an "anticlockwise" response resulted in a shift away from anticlockwise for the next trial. Each staircase thus homed in on the PSV. The test orientations of each staircase were set to a random value between –6 and +6 degrees at the start of the staircase. For the first two trials of each staircase, the step size was ±1.25 degrees and thereafter ±0.35 degrees.

All stimuli were presented in a raised cosine envelope with an exposure duration of 500 ms to minimize the presence of sharp temporal luminance transients. Observers recorded their responses by a key press. Following each response, there was an inter-trial-interval of 500 ms prior to the next stimulus presentation; hence, the observer controlled the timing of stimulus presentation.

Analysis

Data for between four and eight sessions (400–800 trials) were collected for each inducer orientation condition. The data for the + and – inducers for each orientation condition were separately collated and pooled into between five and 10 "bins." Each bin defined a range of test orientations, a mean test orientation, number of trials, and proportion of clockwise responses. The resulting psychometric functions of proportion of clockwise responses as a function of mean test orientation were fitted with Logistic functions to obtain values of PSV_R and PSV_L, defined, respectively, as the test orientations giving 0.5 proportion or 50% clockwise (right) responses for the clockwise and anticlockwise (left) inducers. The PSV for a given inducer orientation condition was then calculated as half the difference between PSV_R and PSV_L, the "halving" serving to facilitate a comparison with PSVs obtained from previous studies employing the single-inducer method. Error bars for each observer were calculated as standard errors derived from bootstrap analysis with 400 iterations. Error bars for the observer averages were calculated as standard errors of the averages. Psychometric function fitting used customized routines from the Palamedes toolbox running under Matlab (Prins & Kingdom, 2018). Figure 2 shows example psychometric functions and illustrates the method for deriving the PSVs.

Results

Experiment 1: Tilt illusion for LM, CM, and OM gratings

The aim of this experiment is to measure the TI for LM, CM, and OM gratings, across the full range of

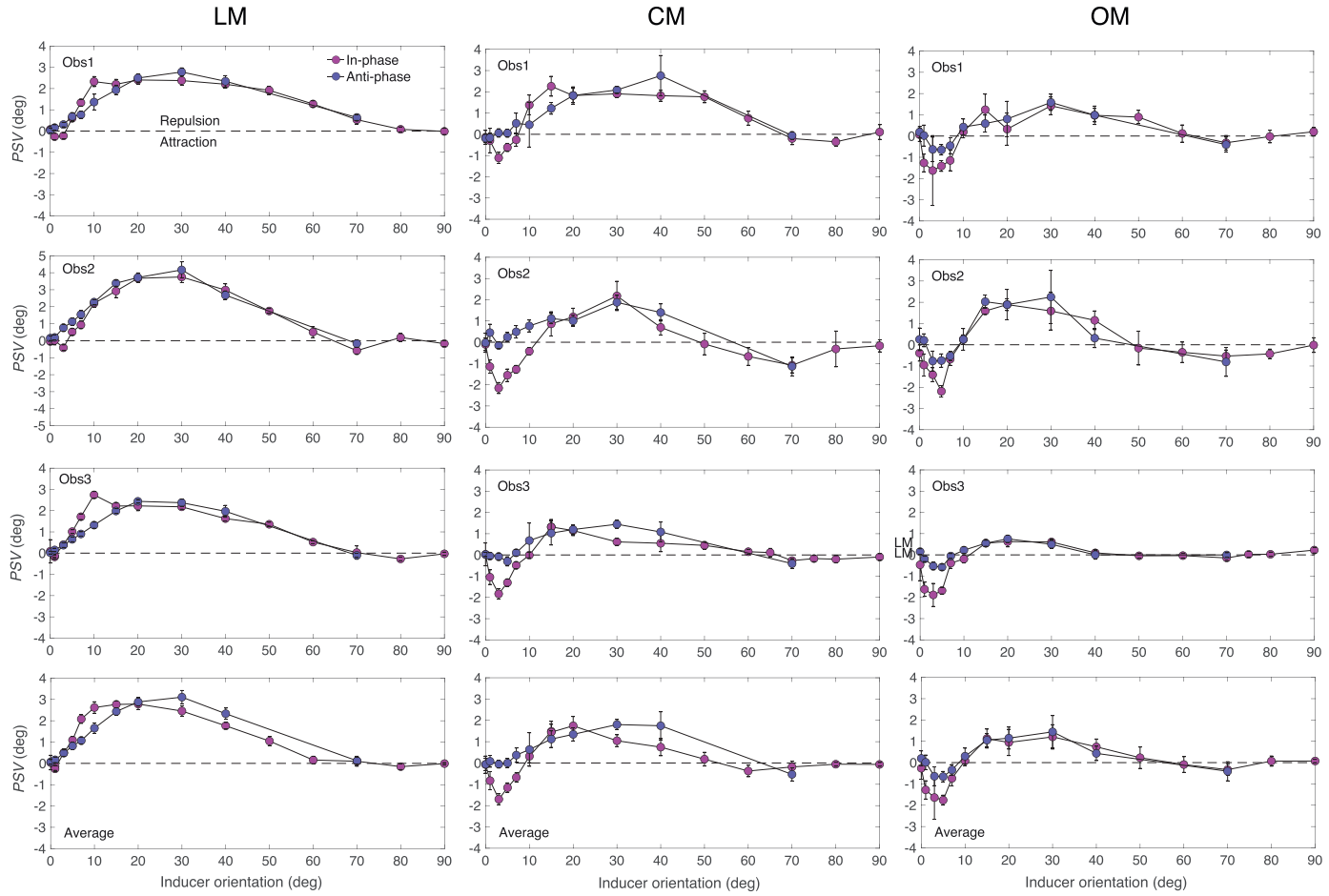

Figure 3. The points of subjective vertical (*PSVs*) as a function of absolute inducer orientation for three observers and in the bottom panels the average across observers, for the luminance-modulated (LM), contrast modulated (CM), and orientation modulated (OM) stimuli. Magenta symbols are for "in-phase" and blue symbols "anti-phase" inducer-test conditions. Positive PSVs show repulsion, and negative PSVs show attraction. Note that the Y-axis range for observer 2's LM data is –5 to +5 degrees compared to the –4 to + 4 degrees range on all other graphs. Small-angle attraction is readily observed in the CM and OM stimuli. Error bars for the individual observers' data are standard errors derived from bootstrap analysis, whereas error bars for the average observer's data are standard errors of the mean.

inducer orientations but with a detailed examination of the 0 to 10 degrees range, for both in-phase and anti-phase inducer-test phase relationships. We used a modulation spatial frequency of 0.66 cpd corresponding to 8 cpi. For the in-phase conditions, the following inducer orientations were used: 0, 1, 3, 5, 7, 10, 15, 20, 30, 40, 50, 60, 70, 80, and 90 degrees, and for observer 3 also 65 and 75 degrees. For the anti-phase conditions, the inducer orientations were 0, 1, 3, 5, 7, 10, 15, 20, 30, 40, and 70 degrees. As we noted earlier, the significance of the inducer-test phase relationship declines with inducer-test angle, hence, the reduced number of anti-phase orientations after the somewhat arbitrary cutoff of 40 degrees, albeit with token inducers of 70 degrees. Figure 3 show the results obtained with the three types of stimuli. In each graph, positive PSVs evidence repulsion and negative PSVs attraction. For all observers and stimulus types, there is clear evidence for the classic TI repulsion effect, with the maximum effect around 15 to 30 degrees. There is a hint of large-angle attraction at around 70 degrees for some stimuli but it is generally very weak, and, in some cases (i.e. LM) non-existent. For both OM and CM, there is robust small-angle attraction for inducer orientations <10 degrees with a maximum effect at about 3 degrees, but no evidence for attraction in this region with the LM stimuli. With the CM stimuli small-angle attraction is found with the in-phase but not anti-phase conditions, whereas with the OM stimuli it is found with both phase conditions, albeit greater with the in-phase condition.

In what follows, we consider three possible reasons for the absence of small-angle attraction with our LM stimuli. First, because our LM stimuli were sinusoidally modulated whereas our CM and OM stimuli were

square-wave modulated. Second, because unlike the LM stimuli, the CM and OM stimuli were constructed from micropatterns. Third, because the "effective" contrast of our LM patterns might have been higher than that of our CM and OM patterns. We test these possibilities in the following three experiments.

Experiment 2: Sine-wave versus square-wave om modulations

If the absence of small-angle attraction in the LM stimulus is a result of using a sine-wave rather than square-wave modulation, one would expect the small-angle attraction effect to disappear with the use of a sine-wave modulated OM stimulus. We chose to test sine-wave OM rather than square-wave LM because of the aliasing problem described earlier with square-wave LM. For this experiment, in addition to the 0.66 cpd modulation spatial frequency used in experiment 1, we also tested at modulation frequencies half and double this value (i.e. at 0.33 cpd and 1.32 cpd).

Figure 4 shows the results for both sine-wave and square-wave OM with 3 degree inducers, the approximate orientation for the maximum small-angle attraction effect. Data for both in-phase and anti-phase conditions are shown as a function of modulation spatial frequency. Results show that small-angle attraction occurs with sine-wave not just square-wave OM modulations, and, for this reason, it seems highly unlikely that the absence of small-angle attraction in the LM stimulus is due to its modulation being sinusoidal rather than square-wave.

Experiment 3: LM versus LM-texture

To test whether the presence of micropatterns in the stimulus promotes small-angle attraction, we compare results obtained with LM and LM-texture stimuli. Figure 5 shows PSVs obtained with in-phase and anti-phase stimuli, for an inducer orientation of 3 degrees, and for three spatial frequencies, 0.33, 0.66, and 1.32 cpd. The two main findings are first that small-angle attraction is evident in all the in-phase LM-texture conditions, and, second, that small-angle attraction is now present in the LM condition at the lowest spatial-frequency of 0.33 cpd. These results suggest that defining the waveform with micropatterns is at least part of the reason for the small-angle attraction revealed in the present study, and that small-angle attraction can be observed in LM stimuli providing spatial frequency is sufficiently low. We will return to a discussion of these findings later.

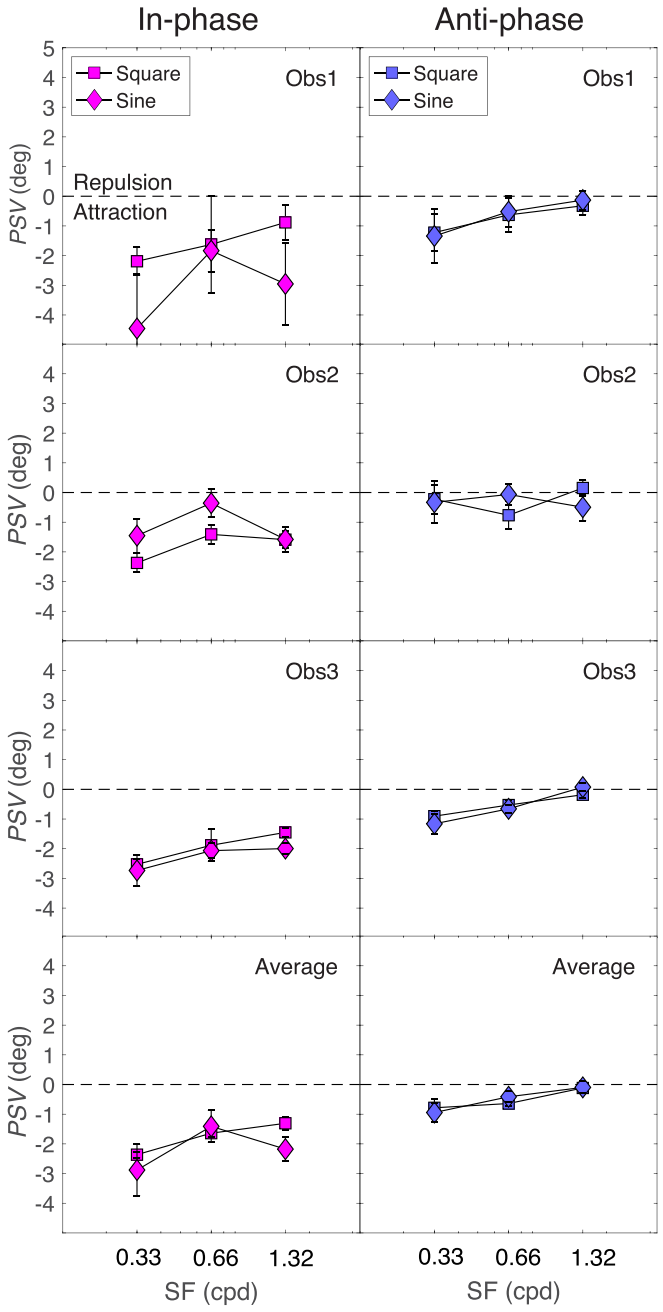

Figure 4. The points of subjective vertical (*PSVs*) for 3 degree inducer square-wave (square symbols) and sine-wave (diamond symbols) OM stimuli as a function of modulation spatial frequency (SF). Left panel/magenta symbols are for in-phase and right panel/blue symbols for anti-phase inducer-test phase relationships. Data are shown for three observers plus their average (bottom panel). Errors on data points for individual observers are standard errors derived from bootstrap analysis, whereas errors for the average data (bottom panels) are standard errors calculated from the observers' *PSVs*.

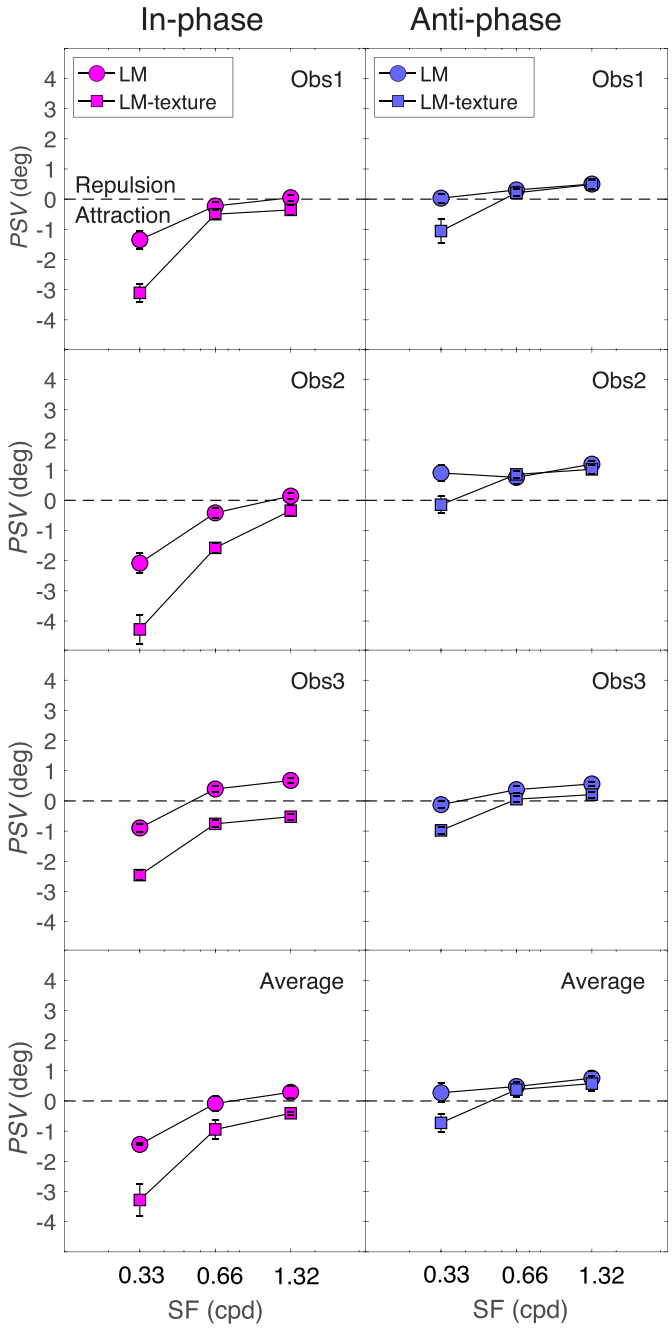

Figure 5. The points of subjective vertical (*PSVs*) for 3 degree inducer LM (round symbols) and LM-texture (square symbols) stimuli as a function of modulation spatial-frequency (SF), for in-phase (left panel/magenta symbols) and anti-phase (right panel/blue symbols) inducer-test phase relationships. Data are for three observers plus their average (bottom panel). Errors are as described in Figure 4.

Experiment 4: LM at low contrast

The third possible reason for the absence of small-angle attraction in our initial LM stimuli is that the LM contrasts were too high in comparison to those used with the CM and OM stimuli. In other words, they were not "equivalent" in terms of their perceived modulation contrast. To test this possibility, we generated LM stimuli with contrasts that were equivalent to those used with the OM stimuli. Intuitively the equivalence should be defined in terms of the task i.e. orientation discriminability. In our experiments, orientation discriminability is measured by the slopes of the psychometric functions, so we determined for each observer the contrast of an LM stimulus that produced the same psychometric function slope as the OM stimulus. We determined these slopes using the same task as in the main experiment, but with the inducer modulation set to zero amplitude, as we found that the slopes were strongly affected by the orientation of above-zero-amplitude inducers. To determine the equivalent LM contrast, we first measured the OM slope using the same test modulation of 0.66 cpd as in the main experiment, then we measured slopes for various LM contrasts. We then used linear interpolation of the LM slope-versus-contrast function to find the slope that matched that of the OM stimulus. The resulting equivalent LM contrasts for observers 1 to 4 were 0.056, 0.025, 0.03, and 0.009. Results for the equivalent LM contrasts, along with the 0.25 contrast LM condition from the first experiment, are shown in Figure 6. Although there is a small degree of variability across observers, there is consistent evidence for the presence of small-angle attraction in in-phase LM stimuli with these (low) equivalent LM contrasts.

Experiment 5: Effect of spatial frequency with the repulsion effect

In experiment 2, using OM stimuli (see Figure 4), we showed that small-angle attraction obtained with the 3 degree inducer orientation declined with increasing modulation spatial frequency. Do we obtain a similar trend for the repulsion effect obtained with a 15 degree inducer orientation? Figure 7 compares the square-wave OM stimulus PSVs obtained for 3 degree (see the left panels; results from Figure 4) with 15 degree inducers. As the figure shows, unlike the 3 degree attraction data, the 15 degree repulsion data shows on average somewhat less decline in TI magnitude with spatial frequency.

Experiment 6: Effect of Gap Width

Previous studies have shown that increasing the width of the gap between the test and the inducer reduces the repulsion effect in the TI (Mareschal & Clifford, 2012). In this experiment, we examine the effect of gap width on both small-angle attraction and repulsion using 3 degree and 15 degree inducer orientations with the OM stimulus. To do this, we measure PSVs as a function

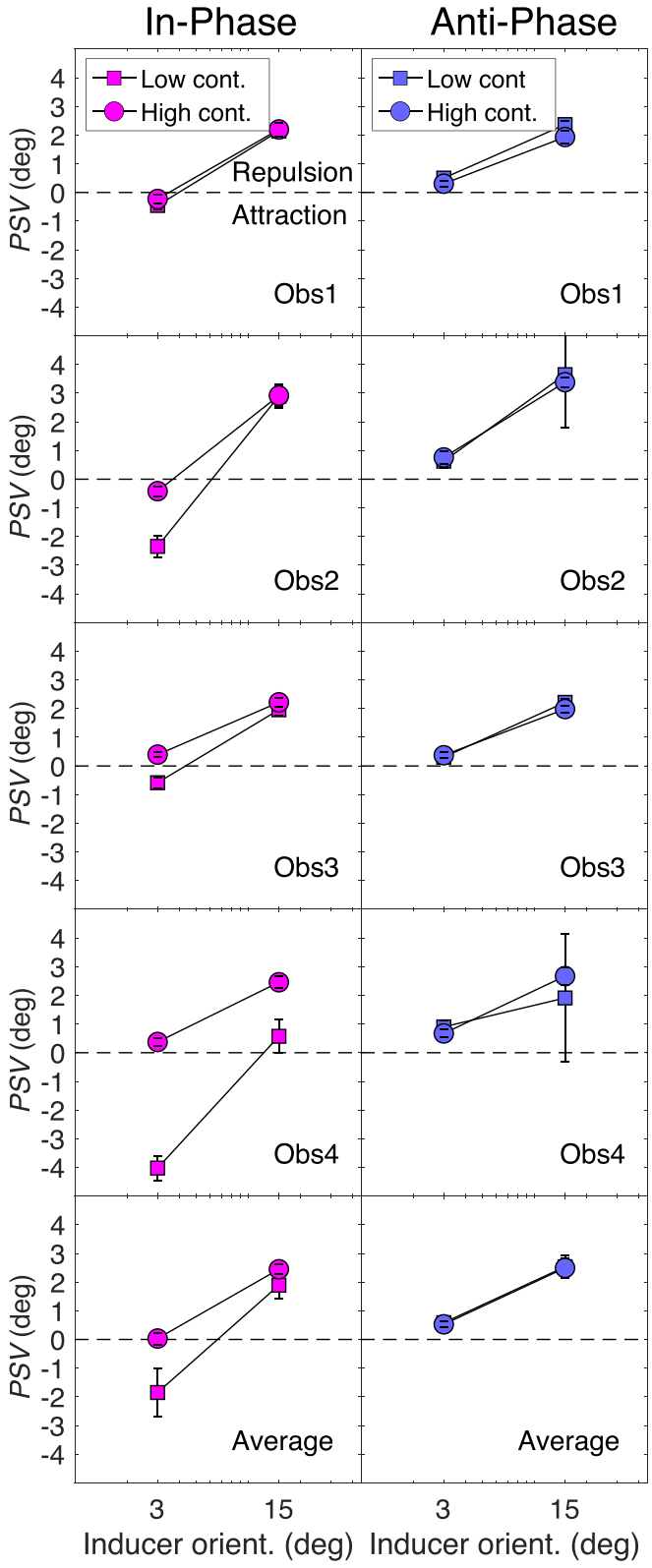

Figure 6. The points of subjective vertical (*PSVs*) for LM stimuli as a function of inducer orientation (orient.), for low "equivalent" contrast (cont.; square symbols) and high contrast (round symbols) in-phase (magenta symbols) and anti-phase (blue symbols) conditions, for four observers plus their average. See the text for further details. Errors are as described for Figure 4.

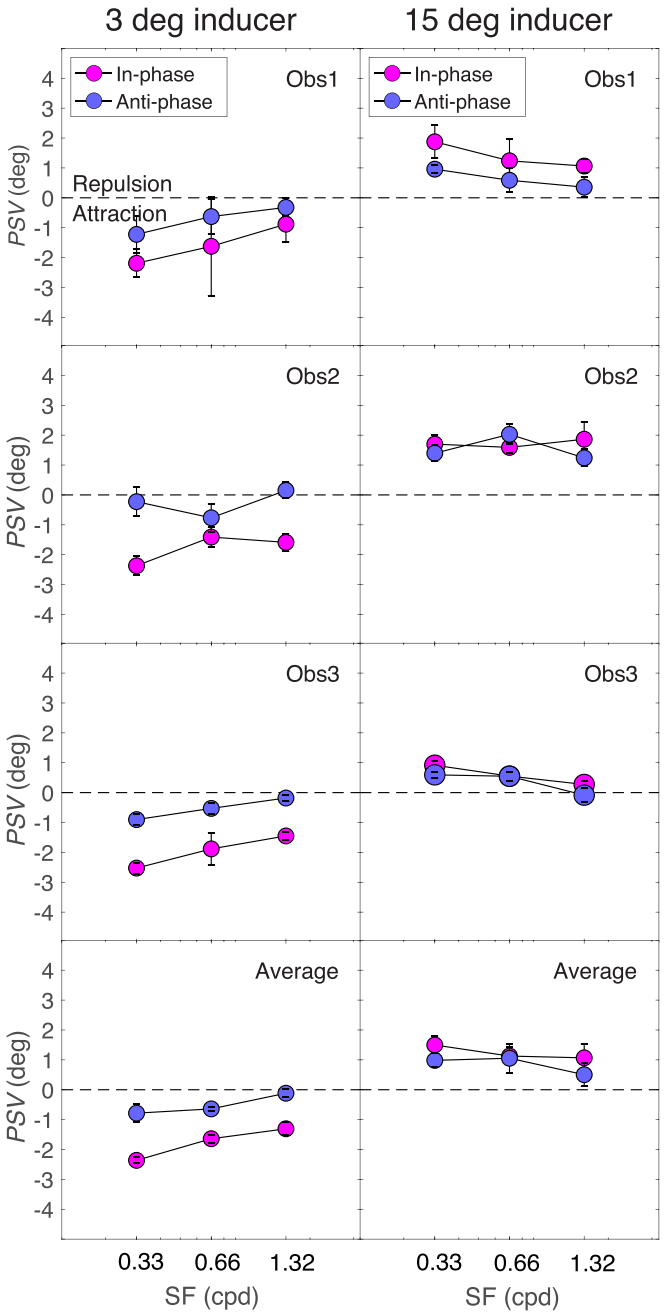

Figure 7. The points of subjective vertical (*PSVs*) for square-wave OM stimuli as a function of modulation spatial frequency (SF), for 3 degree (left panel) and 15 degree (right panel) inducers and for in-phase (magenta symbols) and anti-phase (blue symbols) inducer-test phase relationships, for three observers and their average. Errors are as described for Figure 4.

of gap width for 0.25, 0.5, 0.75, 1, and 2 degree gap size. Results are plotted in Figure 8 and show a similar proportional decline in the TI with increasing gap width for all conditions, with the TI disappearing at a gap width of approximately 1 to 2 degrees.

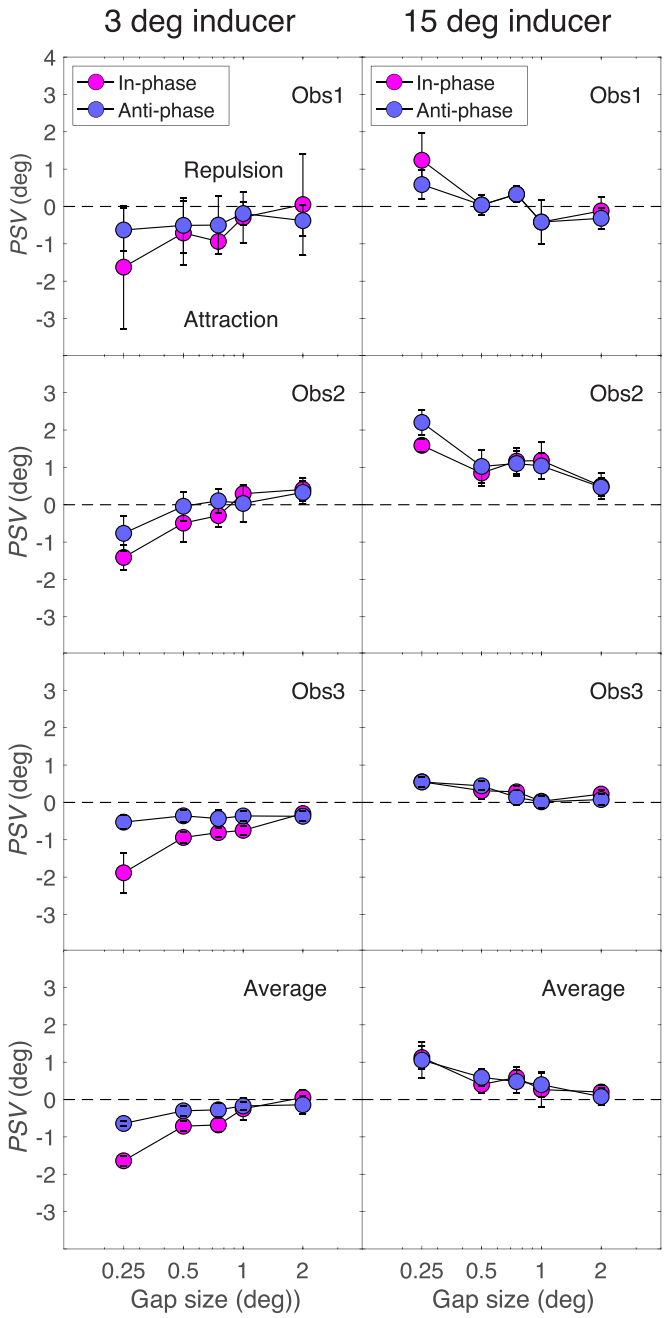

Figure 8. The points of subjective verticality (*PSVs*) with OM stimuli as a function of gap size for 3 degree (left panel) and 15 degree (right panel) inducers, for in-phase (magenta symbols) and anti-phase (blue symbols) inducer-test relationships, and for three observers plus their average (bottom panels). Errors are as described for Figure 4.

Discussion

Small-angle attraction in the tilt illusion

We have demonstrated small-angle attraction in the TI at inducer orientations smaller than 10 degrees in CM, OM, and LM-texture stimuli, and LM stimuli of relatively low-spatial-frequency and/or low contrast. Overall, the magnitude of small-angle attraction (a) was stronger with in-phase compared to anti-phase modulations, (b) for in-phase modulations was as strong or even stronger than the repulsion effect, and (c) decreased with inducer-test gap width and modulation spatial-frequency.

These results complement previous evidence for small-angle attraction in the TI for <= 10 degree inducer-test differences found under very limited circumstances; either only at very short (20 ms) presentation times (Takeo et al., 2020) or when using Gabor test-flanker stimuli at 10 degrees of eccentricity (Mareschal et al., 2010). Our results show that small-angle attraction can be found under more conventional spatio-temporal conditions, albeit best for in-phase inducer-test stimuli.

What mechanism underpins small-angle attraction in the TI? Numerous studies have shown a decline in the TI as the inducer and test orientations approach each other (e.g. see our own results with LM stimuli in Figure 2). This decline speaks to a reduction in the amount of inhibition among inducer and test orientation-selective neurons, as embodied in models of the TI and related phenomena (Clifford, 2014; Clifford, Wenderoth & Spehar, 2000; Motoyoshi & Kingdom, 2003). Although an absence of inhibition is doubtless a pre-condition for small-angle attraction in the TI, it is arguably insufficient. Moreover, it is hard to see how the disinhibition and constancy theories advanced to account for the large-angle attraction effect in the TI (Clifford, 2014; Wenderoth & Johnstone, 1987; Wenderoth & Johnstone, 1988) offer an explanation for its small-angle cousin. Instead, the classical notion of assimilation would seem to offer the best account.

Evidence for assimilation effects in center-surround interactions have been demonstrated in stimulus dimensions other than orientation (e.g. motion; for a review see Tadin & Lapin, 2005), contour-shape (see review by Gheorghiu, Kingdom & Petkov, 2014), color (see review by Kingdom, 2017), and stereo-depth (van der Kooij & te Pas, 2009). Each manifests itself as a shift in the relevant perceived feature of a central test toward that of a surround. Such assimilation effects are likely caused by the surround stimuli falling within the excitatory parts of the neural receptive fields sensitive to the test region. The result is that the population response of the test-sensitive neurons becomes skewed toward those of the neurons sensitive to the inducer, causing the test feature to appear shifted in the direction of the inducer.

Five pieces of evidence attest to an assimilation explanation for small-angle attraction in the TI. First, the anti-phase conditions produced either no or reduced small-angle attraction compared to the in-phase

conditions, presumably because of mutual cancelation of the inducer and test receptive fields in the regions where they overlap. Second, for the fixed-size test area used in the present study, small-angle attraction increased as spatial frequency decreased, consistent with the idea that the larger receptive fields associated with lower spatial frequencies enjoyed a greater degree of inducer-test overlap. Third, in keeping with previous findings by Virsu and Taskinen (1975) and Mareschal and Clifford (2012) in relation to the repulsion effect, small-angle attraction declined markedly with gap size, disappearing altogether between 1 and 2 degrees, as one would expect if the receptive field overlap also declined with increasing gap size. Fourth, although less obvious, is the effect of reducing LM contrast. Remember that the "equivalent" LM contrasts we used were selected to match the orientation discriminability of the OM stimuli, and were very low, ranging from about 1% to 5% across observers, hence barely visible at the low end of the range. At such low contrasts, evidence from single-unit recording of neurons in the macaque have revealed that the size of receptive fields can increase by two to four times their normal size (Kapadia, Westheimer, & Gilbert, 1999; Sceniak, Ringach, Hawken, & Shapley, 1999), a finding that resonates with psychophysical evidence obtained from orientation discrimination in the context of surround masks (Mareschal, Henrie, & Shapley, 2002), as well as center-surround interactions in contour shape perception showing that assimilation of contours into OM textures increases with decreasing center-surround contrast (Gheorghiu & Kingdom, 2019).

Finally, we found that small-angle attraction is greater with LM-texture compared to LM stimuli at all spatial frequencies. This is in keeping with the idea that the presence of micropatterns in the LM-texture stimulus has the effect of broadening the range of orientation and spatial-frequency channels sensitive to the stimulus, thus introducing lower spatial-frequencies with greater inducer-test receptive field overlap.

Whatever happened to large-angle attraction?

One interesting feature of our data is the almost complete absence of the attraction effect typically found with large angles around 70 degrees. Large-angle attraction in the TI has been attributed to disinhibition (Clifford, 2014) and to orientation constancy (Wenderoth & Johnstone, 1987; Wenderoth & Johnstone, 1988; van der Zwan & Wenderoth, 1994; van der Zwan & Wenderoth, 1995; Smith & Wenderoth, 1999), the latter we assume to mean that for inducer orientations close to a cardinal orientation (e.g. horizontal or vertical) the whole stimulus perceptually rotates towards the cardinal direction. The orientation constancy explanation is supported by the finding that because large-angle attraction effects are subject to different spatio-temporal dependencies compared to the repulsion effect, it is likely mediated by higher striate areas where orientation constancy mechanisms are believed to be involved (Wenderoth & Johnstone, 1987; Wenderoth & Johnstone, 1988; van der Zwan & Wenderoth, 1994; van der Zwan & Wenderoth, 1995; Smith & Wenderoth, 1999). Consistent with the orientation constancy account is the evidence from Tomassini and Solomon (2014) that large-angle attraction requires conscious awareness (though see to the contrary findings from the earlier report by Mareschal & Clifford, 2012). The need for conscious awareness to elicit large-angle attraction would be consistent with the reports from our observers that with our interleaved opposite-sign inducers they were unaware of the sign of inducer angle on each trial. In keeping with this explanation is unpublished data from our laboratory showing greater large-angle attraction with TIs obtained using the traditional single-inducer method.

Finally, could orientation constancy account for the small-angle attraction observed here, given that it occurred for inducer orientations close to vertical? We argue not, on the grounds that it fails to explain the pronounced dependency on the spatial-phase relationship between the inducer and test that we observed across conditions, and because small-angle attraction was observed under conditions in which large-angle attraction was almost completely absent.

Conclusion

We have demonstrated the presence of a strong attractive effect in the TI for small inducer-test orientation angles (<10 degrees) in two types of second-order stimuli, namely CM and OM patterns, and in first-order LM stimuli made either from micropatterns or presented at relatively low spatial frequencies or low contrasts. Our measurements of the strength of small-angle attraction in the TI across a range of conditions have suggested that it is an example of the classical notion of assimilation resulting from an overlap in the receptive fields of neurons sensitive to the inducer and test.

Keywords: tilt illusion, surround induction, texture, assimilation

Acknowledgments

Special thanks to Alex Baldwin for suggesting the experiment involving the use of equivalent LM contrasts.

Supported by a National Science and Engineering Research Council of Canada grant #RGPIN-2016-

03915 given to FK and a Leverhulme Trust grant RPG-2016-056 awarded to EG.

Commercial relationships: none.
Corresponding author: Frederick A. A. Kingdom.
Email: fred.kingdom@mcgill.ca.
Address: McGill Vision Research, Department of Ophthalmology, Montréal General Hospital, Cedar Ave. Rm. L11.512, Montréal, Québec, H3G 1A4, Canada.

References

Badcock, D., & Hutchison, H. (1998). Orientation dependent interaction between first- and second-order texture properties. In G. J. Chder (Ed.), *Investigative Ophthalmology and Visual Science Conference (Fort Lauderdale, Florida ed., Vol. 39, pp. s858)*. Association for Research in Vision and Ophthalmology (ARVO).

Blake, R., Holopigian, K., & Jauch, M. (1985). Another visual illusion involving orientation. *Vision Research, 25*(10), 1469–1476.

Blakemore, C., Carpenter, R. H. S., & Georgeson, M. A. (1970). Lateral inhibition between orientation detectors in the human visual system. *Nature, 228*(5266), 37–39.

Clifford, C. W. G. (2014). The tilt illusion: Phenomenology and functional implications. *Vision Research, 104*, 33–11.

Clifford, C. W. G., Wenderoth, P., & Spehar, B. (2000). A functional angle on some after-effects in cortical vision. *Proceedings of the Royal Society of London. Series B: Biological Sciences, 267*(1454), 1705–1710.

Georgeson, M. A. (1973). Spatial frequency selectivity of a visual tilt illusion. *Nature, 245*(5419), 43–45.

Gheorghiu, E., & Kingdom, F. A. A. (2019) Luminance-contrast properties of texture-shape and texture surround suppression of contour shape. *Journal of Vision, 19* (12) 4, 1–14.

Gheorghiu, E., Kingdom, F. A. A., & Petkov, N. (2014). Contextual modulation as de-texturizer. *Vision Research, 104*, 12–23.

Gibson, J. J. (1937). Adaptation, after-effect, and contrast in the perception of tilted lines. II. simultaneous contrast and the areal restriction of the after-effect. *Journal of Experimental Psychology, 20*(6), 553–569.

Graham, N. V. (2011). Beyond multiple pattern analyzers modeled as linear filters (as classical V1 simple cells): Useful additions of the last 25 years. *Vision Research, 51*, 1397–1430.

Kapadia, M. K., Westheimer, G., & Gilbert, C. D. (1999). Dynamics of spatial summation in primary visual cortex of alert monkeys. *Proceedings of the National Academy of Science USA, 96*, 12073–12078

Kingdom, F. A. A. (2017). Color assimilation. In *The Oxford Compendium of Visual Illusions,* by A. Shapiro, & D Todorovic. (Eds.). Oxford, England, UK: Oxford University Press.

van der Kooij, K., & te Pas, S. F. (2009). Perception of 3D shape in context: contrast and assimilation. *Vision Research, 49*, 746–751.

Mareschal, I., & Clifford, C. (2012). Dynamics of unconscious contextual effects in orientation processing. *Proceedings of the National Academy of Science USA, 109*(19), 7553–7558.

Mareschal, I., Henrie, J. A., & Shapley, R. M. (2002) A psychophysical correlate of contrast dependent changes in receptive field properties. *Vision Research, 42*, 1879–1887

Mareschal, I., Morgan, M. J., & Solomon, J. A. (2010). Cortical distance determines whether flankers cause crowding or the tilt illusion. *Journal of Vision, 10*(8) 13, 1–4.

Motoyoshi, I., & Kingdom, F. A. A. (2003). Orientation opponency in human vision revealed by energy-frequency analysis. *Vision Research, 43*, 2197–2205.

Over, R., Broerse, J., & Crassini, B. (1972). Orientation illusion and masking in central and peripheral vision. *Journal of Experimental Psychology, 96*(1), 25–31.

Prins, N., & Kingdom, F. A. A. (2018). Applying the model-comparison approach to test specific research hypotheses in psychophysical research using the Palamedes toolbox. *Frontiers in Psychology, 9*, 1250.

Ringach, D. L. (1998). Tuning of orientation detectors in human vision. *Vision Research, 38*(7), 963–972.

Sceniak, M. P., Ringach, D. L., Hawken, M. J., & Shapley, R. M. (1999). Contrast's effect on spatial summation by macaque V1 neurons. *Nature Neuroscience, 2*, 733–739.

Schofield, A. J., Heese, G., Rock, P. B., & Georgeson, M. A. (2006). Local luminance amplitude modulates the interpretation of shape from shading in textured surfaces. *Vision Research, 46*, 3462–3482.

Smith, S., Clifford, C. W., & Wenderoth, P. (2001). Interaction between first- and second-order orientation channels revealed by the tilt illusion: Psychophysics and computational modelling. *Vision Research, 41*(8), 1057–1071.

Smith, S., & Wenderoth, P. (1999). Large repulsion, but not attraction, tilt illusions occur when stimulus parameters selectively favour either transient (M-like) or sustained (P-like) mechanisms. *Vision Research, 39*(24), 4113–4121.

Tadin, D., & Lappin, J. S. (2005). Linking psychophysics and physiology of center-surround interactions in visual motion processing. In M. R. M. Jenkin, & L. R. Harris (Eds.), *Seeing Spatial Form,* pp. 279–314. Oxford, England, UK: Oxford University Press.

Takeo, S., Watanabe, K., & Clifford, C. W. G. (2020). Angular tuning of tilt illusion depends on stimulus duration. *Vision Research, 175*, 85–89.

Tolhurst, D., & Thompson, P. (1975). Orientation illusions and after-effects: Inhibition between channels. *Vision Research, 15*, 967–972.

Tomassini, A., & Solomon, J. A. (2014). Awareness is the key to attraction: dissociating the tilt illusions via conscious perception. *Journal of Vision, 14*(12), 15.

van der Zwan, R., & Wenderoth, P. (1994). Psychophysical evidence for area v2 involvement in the reduction of subjective contour tilt aftereffects by binocular rivalry. *Visual Neuroscience, 11*(4), 823–830.

van der Zwan, R., & Wenderoth, P. (1995). Mechanisms of purely subjective contour tilt aftereffects. *Vision Research, 35*(18), 2547–2557.

Virsu, V., & Taskinen, H. (1975). Central inhibitory interactions in human vision. *Experimental Brain Research, 23*(1), 65–74.

Wallace, G. K. (1969). The critical distance of interaction in the Zöllner illusion. *Perception & Psychophysics, 5*(5), 261–264.

Wenderoth, P., & Johnstone, S. (1987). Possible neural substrates for orientation analysis and perception. *Perception, 16*(6), 693–709.

Wenderoth, P., & Johnstone, S. (1988). The different mechanisms of the direct and indirect tilt illusions. *Vision Research, 28*(2), 301–312.